Supplementary Material

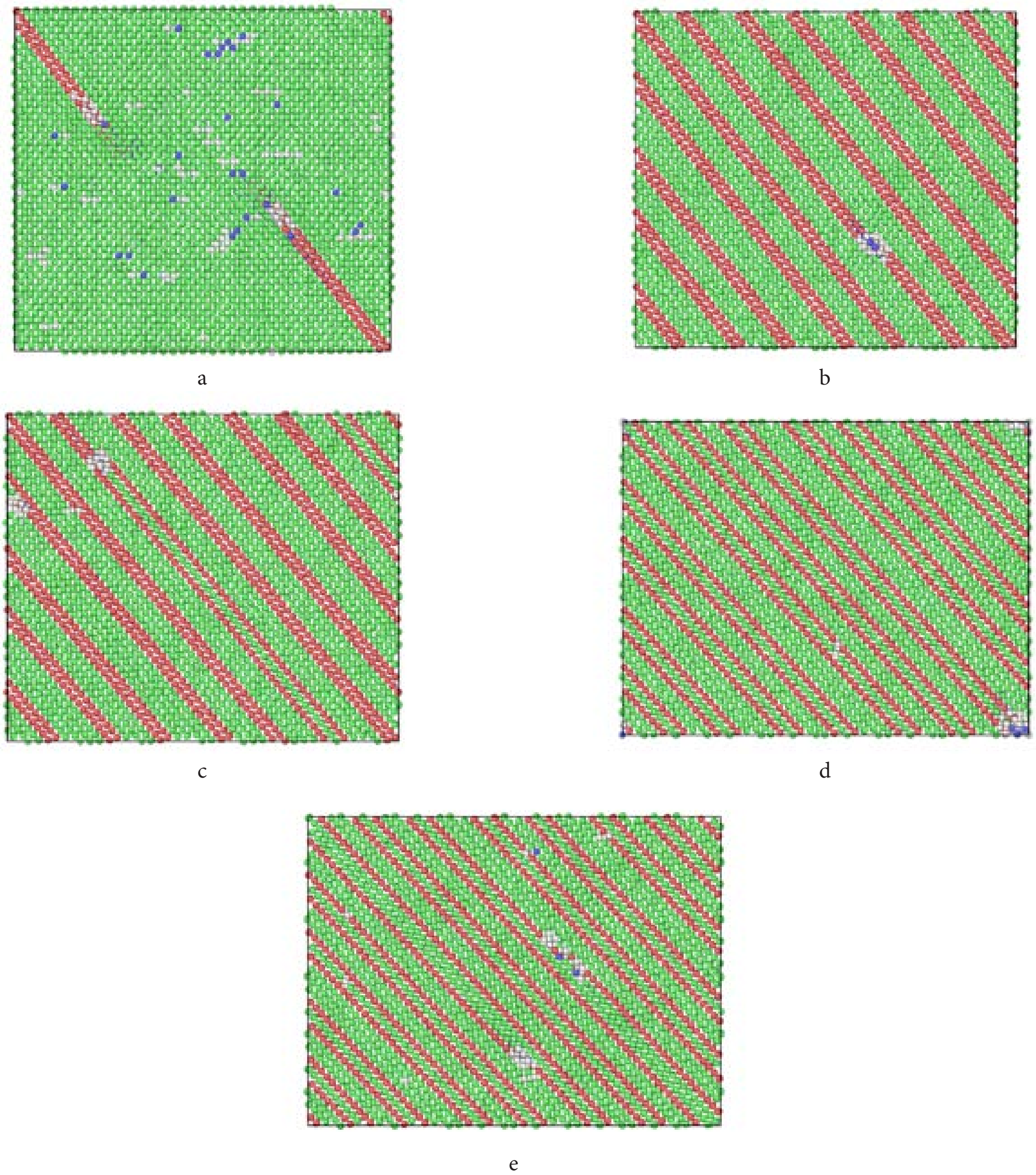

Fig. S1. Structure of the $Fe_{30}Mn_{30}$-sample in projection on the $(\bar{1}10)$ plane for tension at a rate of 10^8 s^{-1} to a value of: 0.0525 (a), 0.068 (b), 0.0975 (c), 0.14 (d), 0.1575 (e). Green, red, blue, and grey colors of the atoms denote fcc, hcp, bcc and undefined symmetries of their nearest-neighbor environment, respectively.

In the process of tension at $\dot{\varepsilon}=10^9$ s^{-1}, in 4 cases out of 5, several SFs nucleate in the $Fe_{30}Mn_{30}$-sample rather than one. The loading diagram in these cases (Fig. S2) does not differ much from the one shown in Fig. 1a, but due to the intersection of SFs (Fig. S3a, b) there forms a totally different system of defects. After the first stress unloading, the growth of stresses stops at $\varepsilon=0.1$, when in the regions between the SFs new SFs nucleate homogeneously (Fig. S3c) — first the fraction of undefined and bcc atoms grows, and then the fraction of hcp atoms grows as well (Fig. S2). In a range of $\varepsilon=0.100-0.121$ new SFs intersect the old ones (Fig. S3d), transform into extrinsic SFs, and a twin forms throughout the whole sample length in the $(\bar{1}\bar{1}1)$ plane (Fig. S3e), which leads to a considerable decline in stress. By $\varepsilon=0.160$ three-layer bands with an hcp lattice have formed (Fig. S3f). Then the short fragments of SFs annihilate, and the thickness of the hcp bands is 3 to 5 atomic layers (Fig. S3g). The regions of intersection of the hcp bands and SFs become arranged into two planes perpendicular to the tension direction, forming walls from the 1/6 <112> partial dislocations. They can be regarded as grain boundaries, because crystalline lattices change orientation when passing through them.

DOI: 10.22226/2410-3535-2018-3-311-316

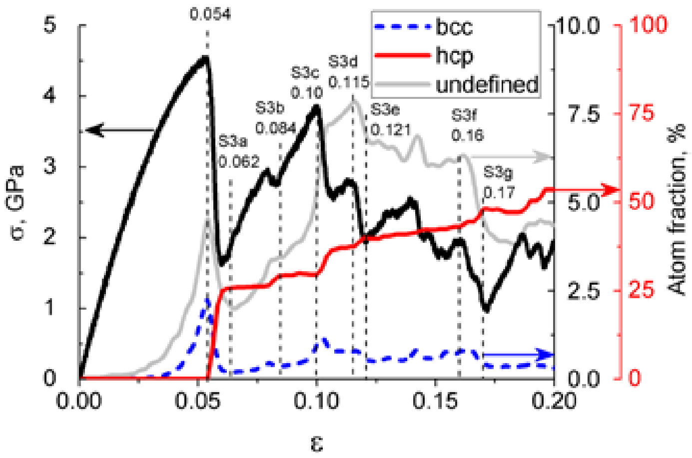

Fig. S2. Stress along the [110] direction (left axis) and the fraction of bcc, hcp and undefined atoms versus strain (right axes) for the tension of the $Fe_{30}Mn_{30}$-sample at a rate of 10^9 s^{-1} in the case of nucleation of several stacking faults.

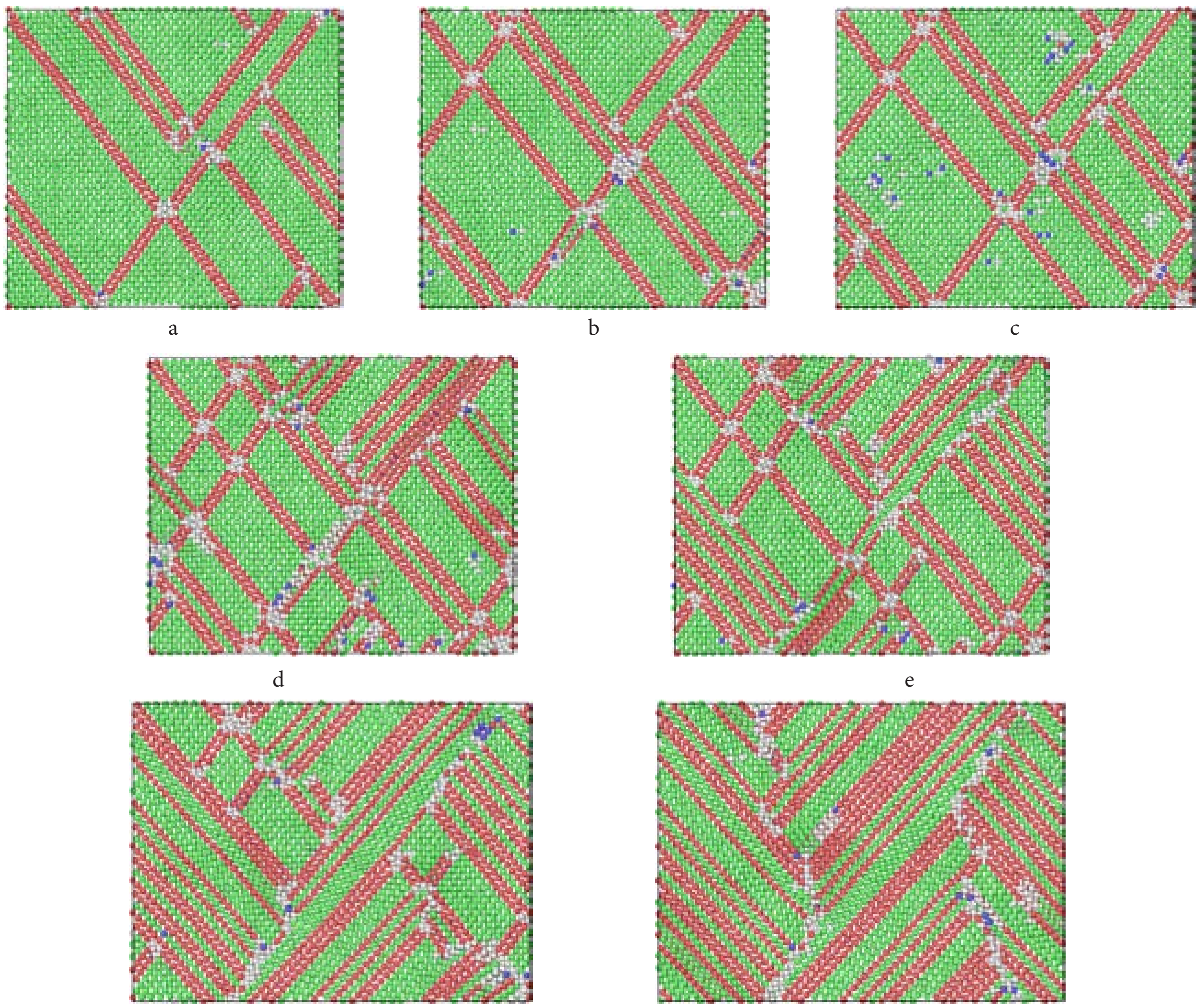

a b c d e f g

Fig. S3. Structure of the $Fe_{30}Mn_{30}$-sample in projection on the $(\bar{1}10)$ plane for tension at a rate of 10^9 s^{-1} to a value of: 0.062 (a), 0.084 (b), 0.10 (c), 0.115 (d), 0.125 (e), 0.16 (f), 0.17 (g). The designation of atoms by colors is the same as in Fig. S1.

DOI: 10.22226/2410-3535-2018-3-311-316

At the first unloading of tensile stresses (Fig. S4) for $\dot{\varepsilon} = 10^9$ s^{-1} plasticity in the $Co_{30}Cr_{30}$-sample and in the $Fe_{30}Mn_{30}$-sample develops in the same manner: two SFs nucleate (Fig. S5a), they intersect each other, and by $\varepsilon = 0.074$ one of them has become an extrinsic SF (Fig. S5b). In a range of $\varepsilon = 0.128 - 0.130$ in the whole sample there forms a network of intersected SFs (Fig. S5c) and an hcp band with a thickness of 6 atomic layers, passing through the whole sample. In one of its regions, partial dislocations form a twin. It starts to grow, while the position and sizes of the other defects remain almost unchanged (Fig. S5d). The stress, the quantity of hcp, bcc and undefined atoms practically does not vary (Fig. S4). At $\varepsilon = 0.20$ the twin has a thickness of 6 atomic layers (Fig. S5e).

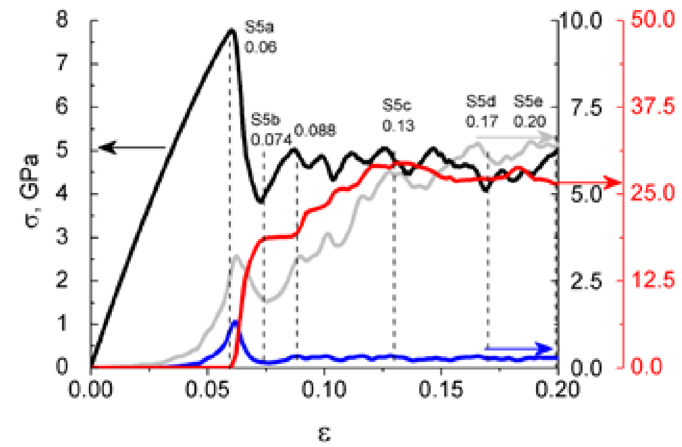

Fig. S4. Stress along the [110] direction (left axis) and the fraction of bcc, hcp and undefined atoms versus strain (right axes) for the tension of the $Co_{30}Cr_{30}$-sample at a rate of 10^9 s^{-1}.

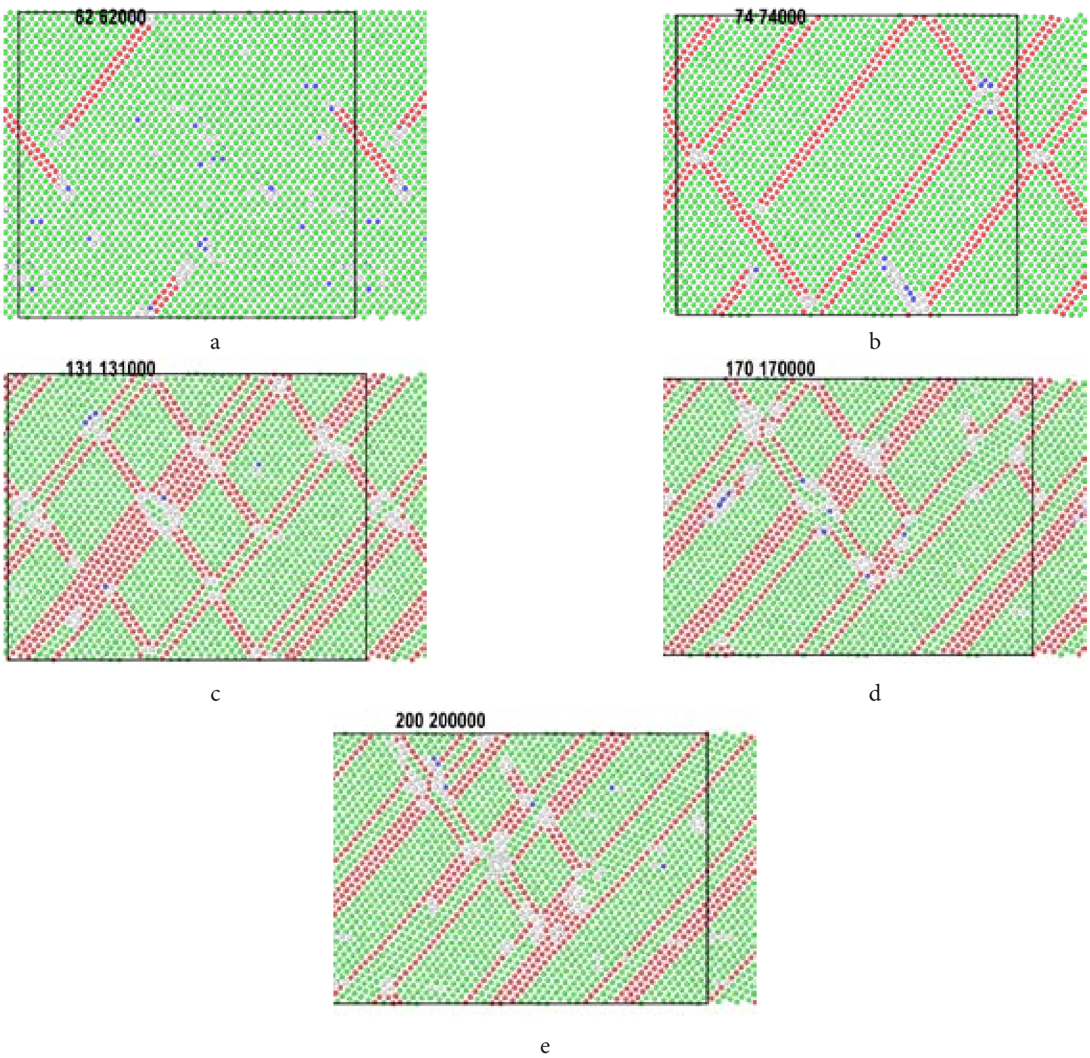

Fig. S5. Structure of the $Co_{30}Cr_{30}$-sample in projection on the $(\bar{1}10)$ plane for tension with a rate of 10^9 s^{-1} to a value of: 0.062 (a), 0.074 (b), 0.131 (c), 0.17 (d), 0.20 (e). The designation of atoms by colors is the same as in Fig. S1.

DOI: 10.22226/2410-3535-2018-3-311-316

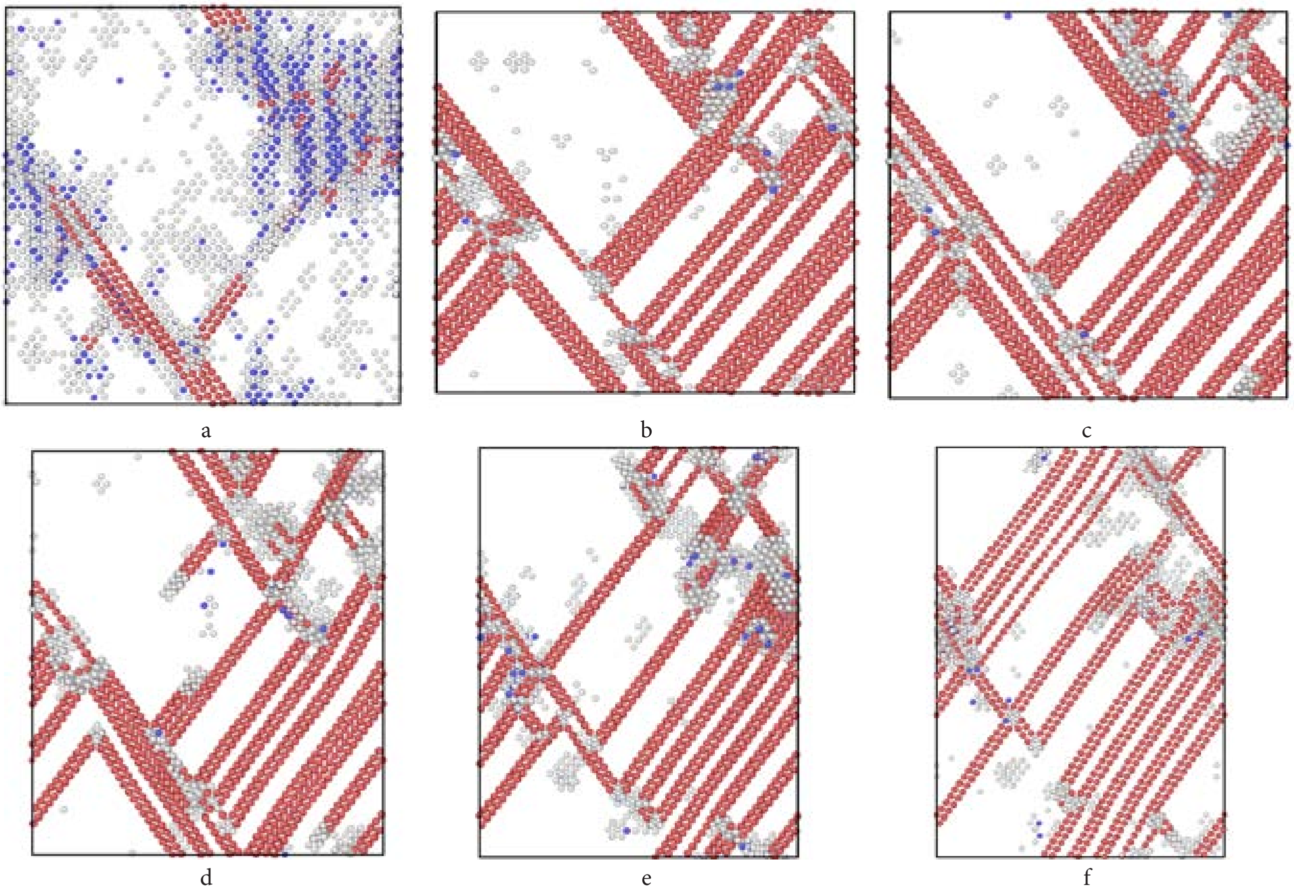

Fig. S6. Structure of the Fe30Mn30-sample in projection on the ($\bar{1}10$) plane for compression with a rate of 10^8 s^{-1} to a value of: 0.06 (a), 0.077 (b), 0.083 (c), 0.105 (d), 0.15 (e), 0.02 (f). The designation of the atoms by colors is the same as in Fig. S1.

During the compression of the $Fe_{30}Mn_{30}$-sample at a rate of $\dot{\varepsilon}=10^9$ s^{-1}, just like at a rate of 10^8 s^{-1}, there form SFs and bands with an hcp lattice (Fig. S8a, b). Although the thickness of the bands is larger (4 – 6 atomic planes), the total fraction of hcp atoms is slightly lower than at $\dot{\varepsilon}=10^8$ s^{-1} (Fig. S7). It further changes only slightly, the stress grows. In the regions of intersection of SFs and bands with an hcp lattice, the lattice becomes more and more distorted, the quantity of atoms with an undefined nearest-neighbor symmetry increases (Fig. S8c). The first stress unloading at the compression of 0.118 is related to the transformation of hcp bands into extrinsic SFs (Fig. S8d), and by 0.138 the thickness of the hcp bands has increased even a little more (Fig. S8e). Note should be made that the regions of intersection of hcp bands are the regions with an hcp lattice, re-oriented with respect to the bands themselves, and often divided from them by {10 – 11} twin boundaries. The {0001} basal planes in the regions of intersection of bands make up an angle of 0 or 90 degrees to the sample's directions of compression and tension. Since in case of the bands, shear is realized in those planes, and further loading of the sample leads to a disordering of the structure in the regions of bands intersection (Fig. S8f). As this happens, a significant drop of stresses occurs.

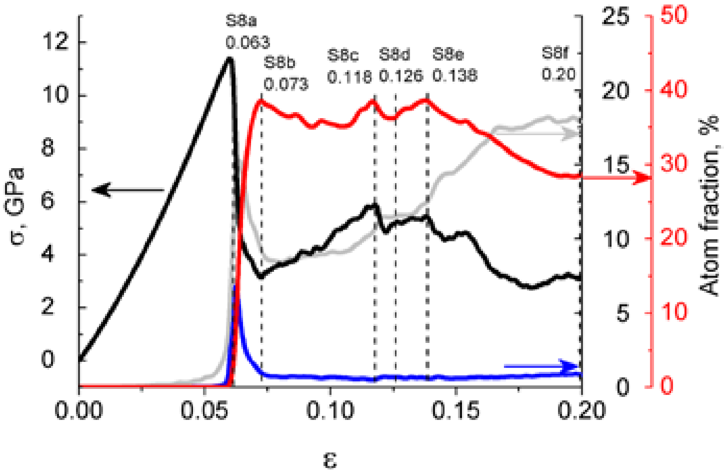

Fig. S7. Stress along the [110] direction (left axis) and the fraction of bcc, hcp and undefined atoms versus strain (right axes) for the compression of the $Fe_{30}Mn_{30}$-sample at a rate of 10^9 s^{-1}.

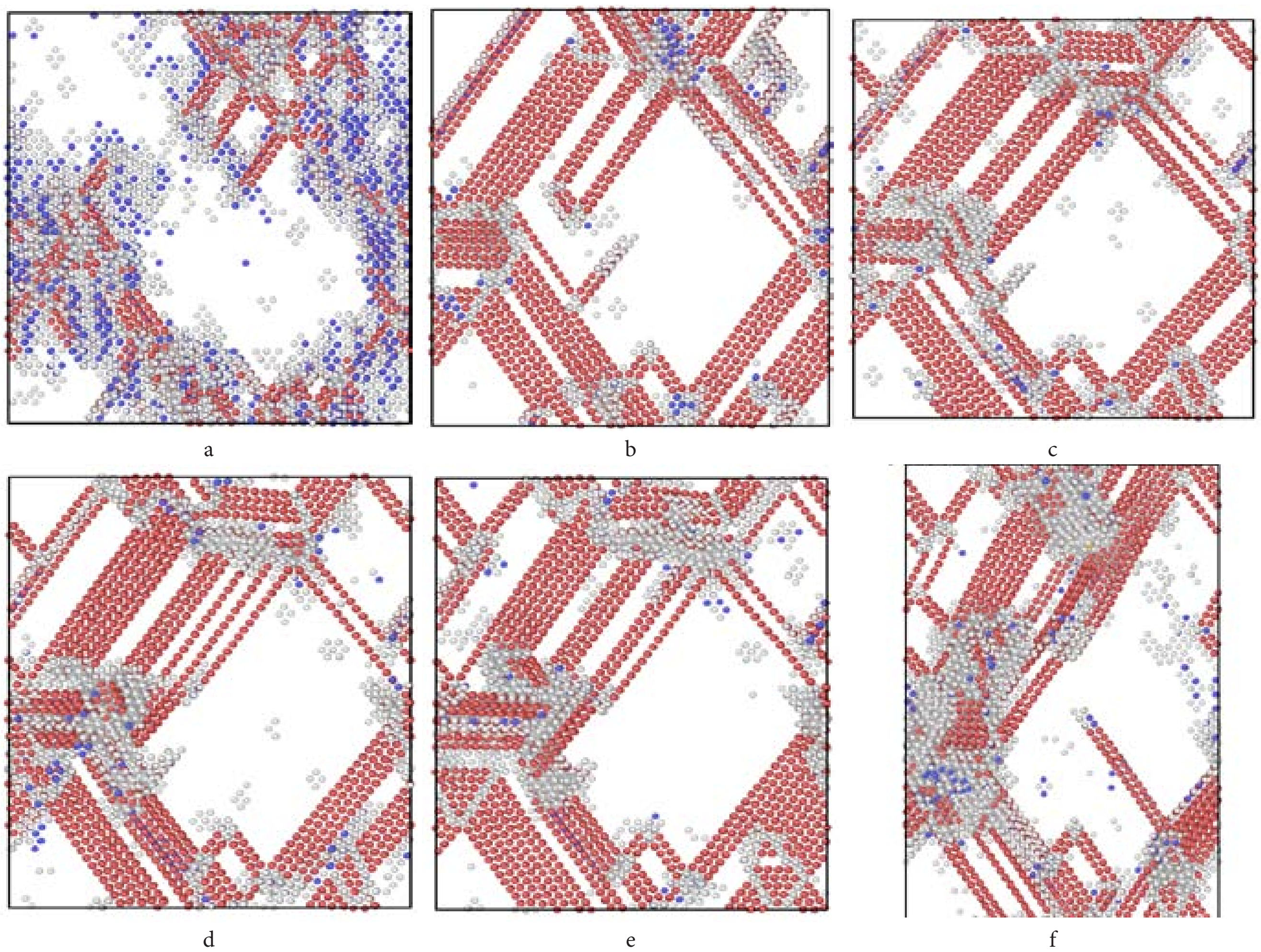

Fig. S8. Structure of the $Fe_{30}Mn_{30}$-sample in projection on the $(\bar{1}10)$ plane for compression at a rate of 10^9 s^{-1} to a value of: 0.063 (a), 0.073 (b), 0.118 (c), 0.126 (d), 0.138 (e), 0.02 (f). The designation of atoms by colors is the same as in Fig. S1.

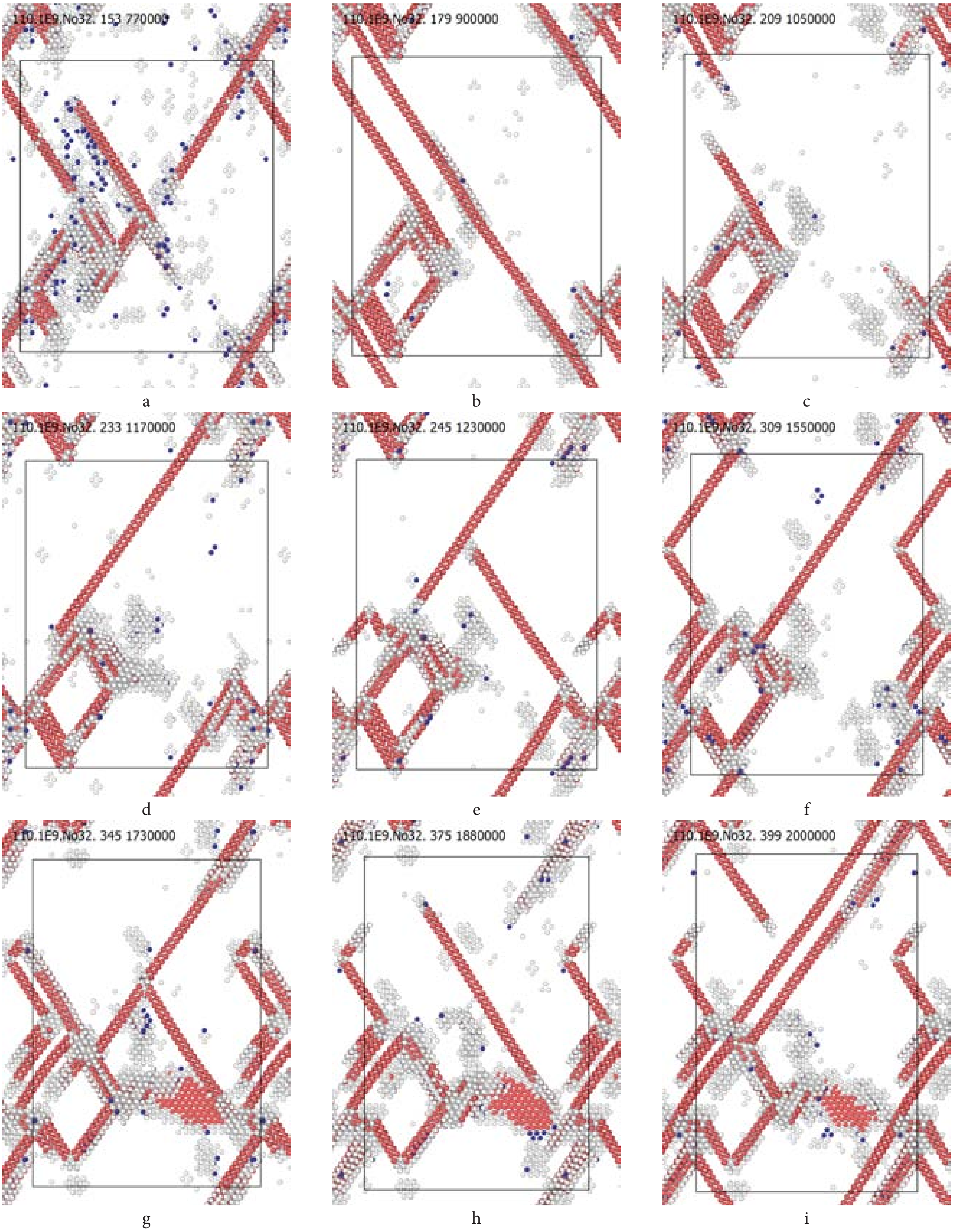

Fig. S9. Structure of the $Co_{30}Cr_{30}$-sample in projection on the $(\bar{1}10)$ plane for compression at a rate of 10^8 s^{-1} to a value of: 0.077 (a), 0.09 (b), 0.1058 (c), 0.117 (d), 0.123 (e), 0.155 (f), 0.173 (g), 0.188 (h), 0.20 (i). The designation of atoms by colors is the same as in Fig. S1.

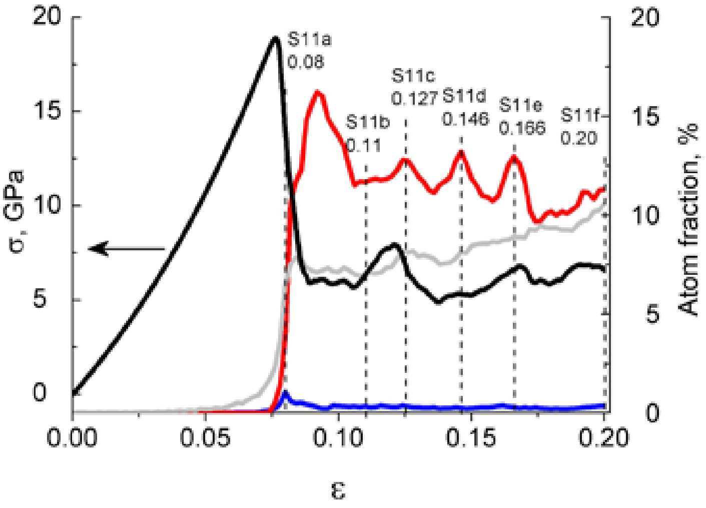

Fig. S10. Stress along the [110] direction (left axis) and the fraction of bcc, hcp and undefined atoms versus strain (right axes) for the compression of the $Co_{30}Cr_{30}$-sample at a rate of 10^9 s^{-1}.

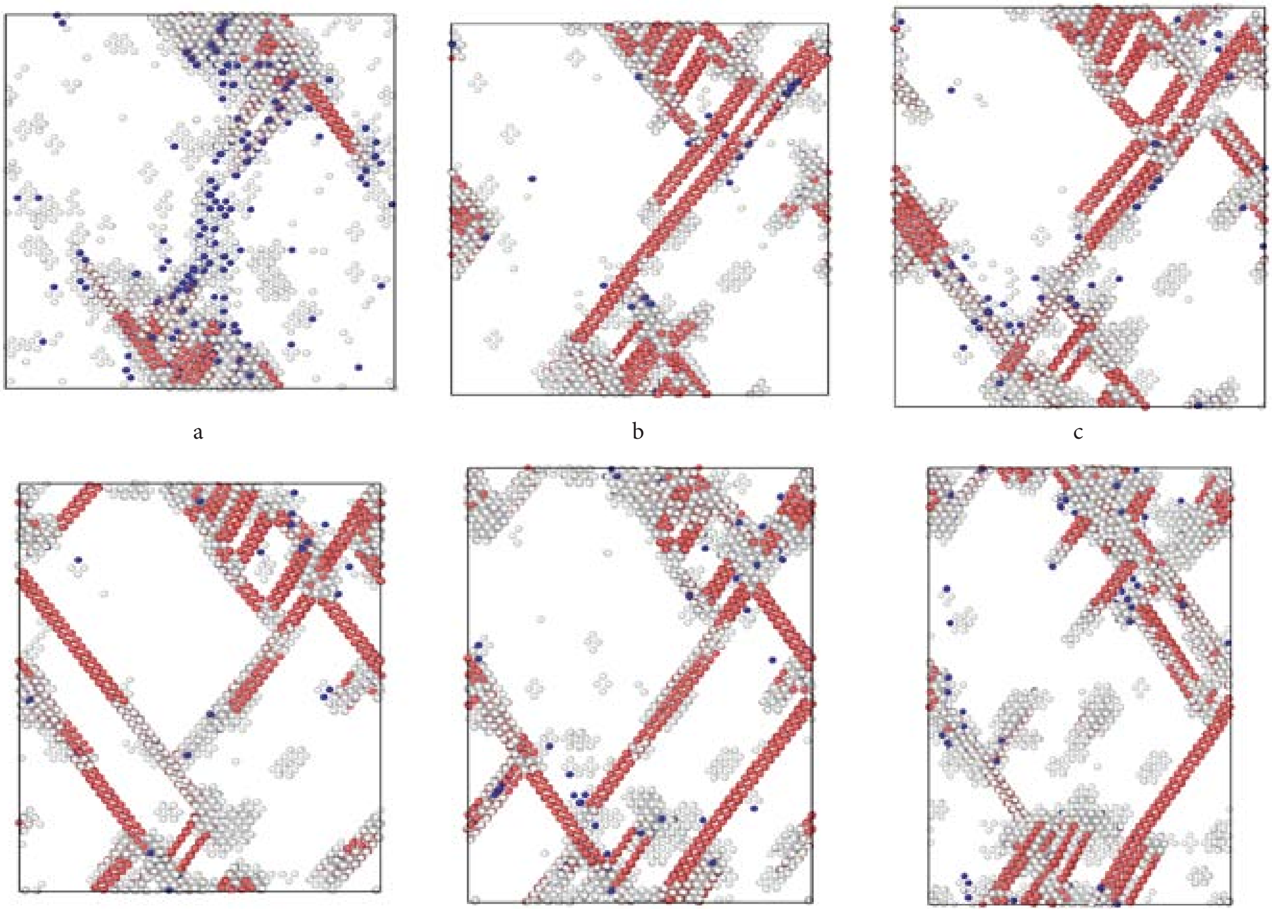

a b c

d e f

Fig. S11. Structure of the $Co_{30}Cr_{30}$-sample in projection on the $(\bar{1}10)$ plane for compression at a rate of 10^9 s^{-1} to a value of: 0.08 (a), 0.11 (b), 0.127 (c), 0.146 (d), 0.166 (e), 0.20 (f). The designation of atoms by colors is the same as in Fig. S1.

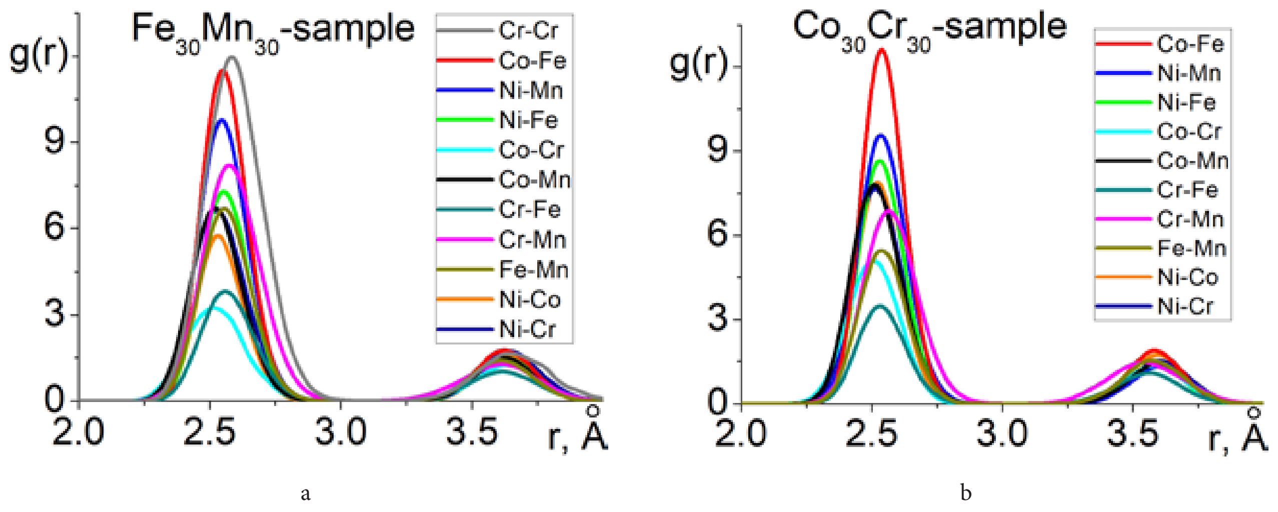

Fig. S12. Radial distribution functions for pairs of chemical elements in the $Fe_{30}Mn_{30}$-sample (a) and in the $Co_{30}Cr_{30}$-sample (b).

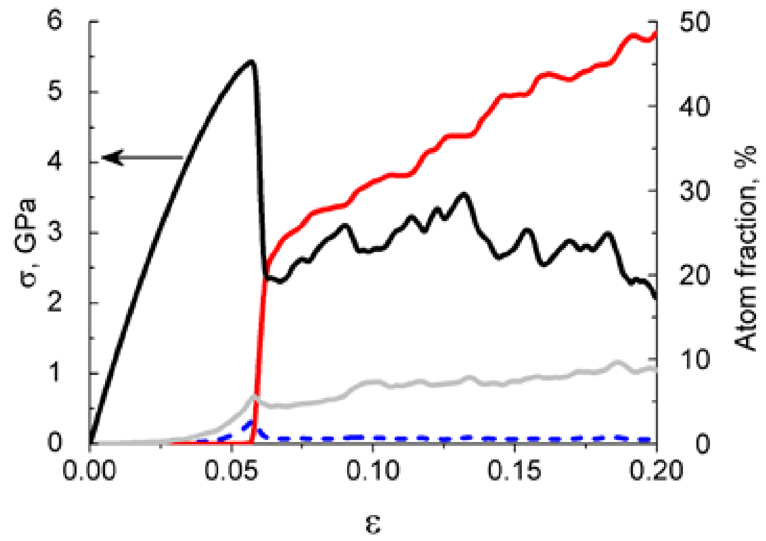

Fig. S13. Stress along the [110] direction (left axis) and the fraction of bcc, hcp and undefined atoms versus strain (right axes) for the tension of the equiatomic sample at a rate of 10^9 s^{-1}.

DOI: 10.22226/2410-3535-2018-3-311-316

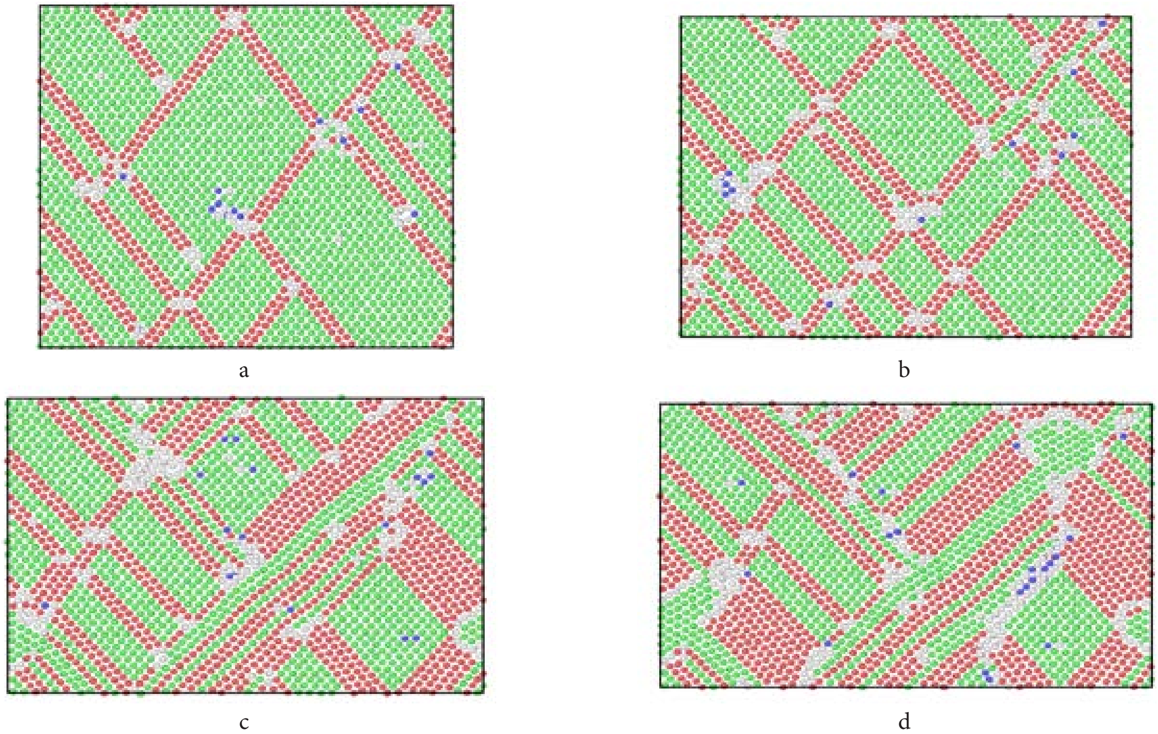

Fig. S14. Structure of the equiatomic sample in projection on the $(\bar{1}10)$ plane for tension at a rate of 10^9 s^{-1} at a value of: 0.07 (a), 0.10 (b), 0.16 (c), 0.17 (d), 0.20 (e). The designation of atoms by colors is the same as in Fig. S1.

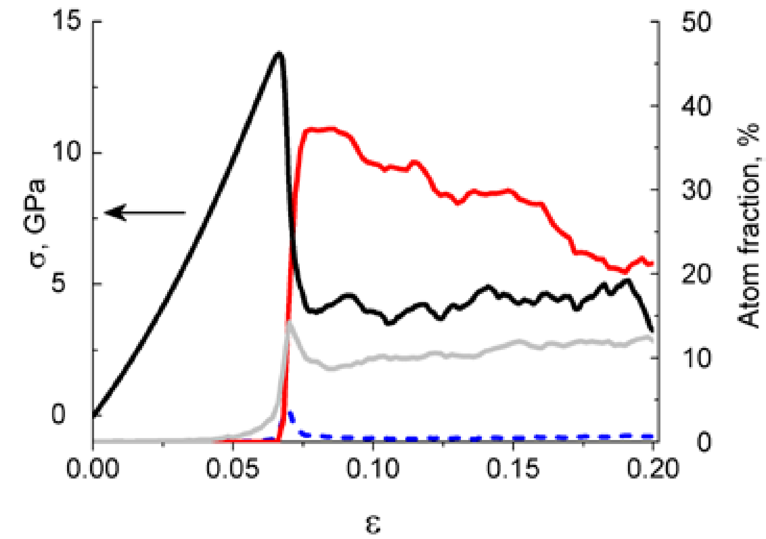

Fig. S15. Stress along the [110] direction (left axis) and the fraction of bcc, hcp and undefined atoms versus strain (right axes) for the compression of the equiatomic sample at a rate of 10^9 s^{-1}.

DOI: 10.22226/2410-3535-2018-3-311-316

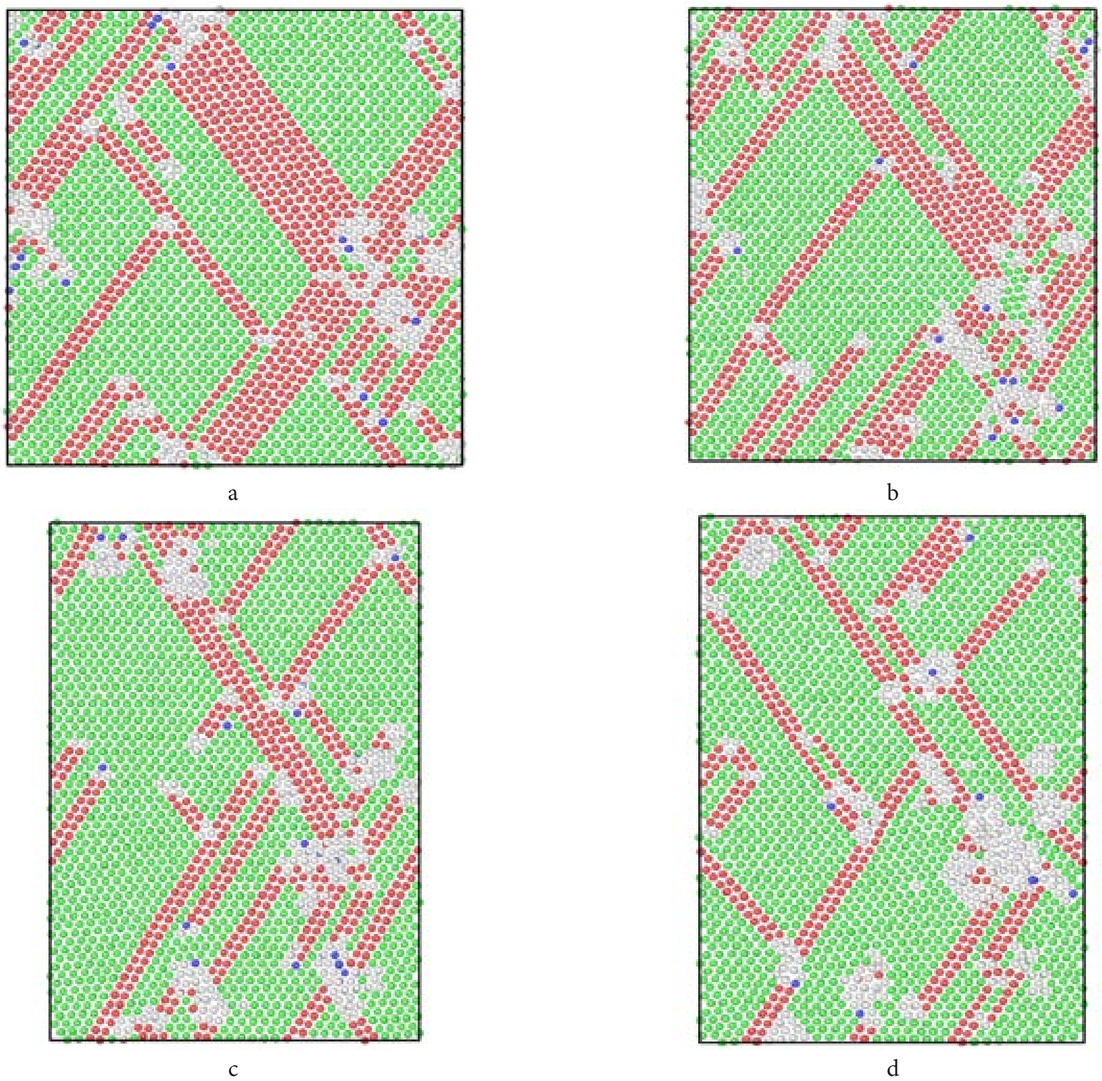

Fig. S16. Structure of the equiatomic sample in projection on the $(\bar{1}10)$ plane for compression at a rate of 10^9 s^{-1} to a value of: 0.08 (a), 0.11 (b), 0.175 (c), 0.20 (d). The designation of atoms by color is the same as in Fig. S1.